Journal of Ceramic Processing Research. Vol. 7, No. 1, pp. 10~13 (2006)

JOURNAL OF
Ceramic Processing Research

Photocatalytic activity of ZrO_2-doped TiO_2 catalysts prepared by a surfactant-assisted templating method

Singto Sakulkhaemaruethai, Athapol Kitiyanan and Susumu Yoshikawa*
Institute of Advanced Energy, Kyoto University, Gokasho, Uji, Kyoto 611-0011, Japan

ZrO_2-doped TiO_2 nanocrystals were prepared by a surfactant-assisted templating method (SATM) under a sol-gel process. Mesoporous anatase-type ZrO_2-doped TiO_2 nanocrystals with a surface area of 40-80 m^2/g were obtained. A small amount of ZrO_2 addition to TiO_2 nanocrystals increased the thermal stability of the anatase phase of TiO_2. By using a photocatalytic reaction of triiodide (I_3^-) ions formation in KI solution by UV-irradiation, it was found that the 0.5 mol% ZrO_2-doped TiO_2 nanocrystals possessed the best photocatalytic activity of the TiO_2-ZrO_2 nanocrystals tested in this study. The effects of calcination temperature and zirconia content on the photocatalytic activity of titania-based nanocrystals were investigated.

Key words: Titania, Photocatalytic activity, Surfactant-assisted templating method, Anatase

Introduction

Nanostructured titania (TiO_2) materials have been the subject of a great deal of research because of their properties and applications in photocatalysis, solar energy conversion, electronic devices, cosmetics, environmental purification, etc. [1-4]. TiO_2 has been widely utilized as a photocatalyst because it is relatively safe, inexpensive and stable to photocorrosion. Oxidation cleavages, condensation, polymerization, geometric and valence isomerization, and substitutions, have been accomplished through photocatalysis with TiO_2 [5-8]. Recently, Karunakaran *et al.* [9] have been studied the photocatalytic activity of TiO_2 by photooxidation of iodide ion. The results showed the catalytic efficiency for the formation of iodine in a TiO_2 photocatalyst aqueous ethanol suspension. The efficiency of the catalyst depends mainly on the intensity of absorbed photons during illumination, the formation of electron-hole pairs and recombination rates, the charge transfer rate, and the reaction conditions [10, 11]. The photocatalytic activity has been improved by optimizing the nanostructure of TiO_2, using various processing routes, such as inert gas condensation [12], a sol-gel method [13, 14], and hydrothermal processing [15]. The photocatalytic activity can also be altered by doping with a transition metal oxide such as ZrO_2 [16], WO_3 [17], etc.; the addition of metal or metal oxide enhances the thermal stability of the anatase phase, and increases the surface area and surface acidity, resulting in improved photocatalytic activity [18-20].

*Corresponding author:
Tel : +81-774-38-3502
Fax: +81-774-38-3508
E-mail: s-yoshi@iae.kyoto-u.ac.jp

In our previous study, mesoporous TiO_2 and ZrO_2-doped TiO_2 nanocrystals have been successfully prepared by a surfactant-assisted templating method (SATM) [21, 22]. By using this method, mesoporous materials with controlled and well-defined pore-structures can be fabricated. The addition of ZrO_2, improved the thermal stability of the metastable anatase phase, which has a better photocatalytic activity than the rutile phase [23]. In this paper, more detailed and further experimental results on the photocatalytic activity of mesoporous ZrO_2-doped TiO_2 nanocrystals will be presented.

Experimental Procedure

All chemicals were analytical grade and used without further purification. The ZrO_2-doped TiO_2 nanocrystals were prepared by SATM [21, 22, 24]. Tetra(*i*-propyl) orthotitanate (TIPT, Tokyo Chemical Industry Co., Japan), acetylacetone (ACA, Nacalai Tesque, Inc., Japan), and laurylamine hydrochloride (LAHC, Tokyo Chemical Industry Co., Japan) were used as TiO_2 precursor, modifying agent, and templating structures, respectively. Zirconyl nitrate hydrate ($ZrO(NO_3)_2$, Aldrich) was used as ZrO_2 precursor. An LAHC solution (0.1 M) containing the appropriate amount of zirconia precursor was mixed with the equimolar mixture of TIPT and ACA and magnetically stirred at room temperature for 1 h. The resulting mixture was further stirred in an oven at 40°C for 24 h. Then, the homogeneous sol was kept sealed at 80°C. After 72 h, the gel obtained was washed with 2-propanol (Nacalai Tesque, Inc., Japan) and dried at 80°C overnight. Finally, the templates were removed from the TiO_2 framework by a calcination process.

Characterization of titania nanocrystals

Transmission electron microscopy (TEM) and selected area electron diffraction (SAED) were performed on a transmission electron microscope (JEOL JEM-200CX) at 200 kV. The X-ray diffraction (XRD) analysis was performed on a micro X-ray diffractometer (Model RINT-2100, Rigaku) with Cu-Kα radiation (λ=0.154 nm) at 40 kV and 40 mA, and a scan rate of 2º(2θ)/minute. The N_2 adsorption-desoprtion isotherms were obtained with a nitrogen adsorption apparatus (BELSORP18 PLUS). The powders were further degassed under vacuum at 200°C for 2 h before measurements to evacuate the physisorbed moisture. Diffuse reflectance spectra were recorded on a UV-vis spectrophotometer (UV-2450 Spectrophotometer, Shimadzu). $BaSO_4$ was used as the reference powder. The collected relative reflection intensity ($R_\infty=R_{sample}/R_{reference}$) was transformed into $F(R_\infty)$ by using the Kubelka-Munk function $F(R_\infty) = (1-R_\infty)^2/(2R_\infty)$ [25]. All spectra were plotted in terms of $F(R_\infty)$ vs. wavelengths. The extrapolation of the absorption edge to the wavelength axis gives the photon energy (E_{phot}) as $E_{phot} = (1239/\lambda)$ eV, where λ is wavelength (in nm). The value of E_{phot} corresponds to the band gap energy [26]. The photocatalytic activity was investigated by adding 50 mg of sample powder into 10 ml, 0.2 M KI aqueous solution in a cylinder reactor. The suspension was magnetically stirred and photoirradiated with a UV lamp (15 W, Vilber Lourmat VL-115L, with a maximum emission at about 365 nm). The concentration of liberated I_3^- ions in the clear supernatant after diluting ten times was monitored at regular time intervals by determining the absorbance at 288 nm, using an UV-vis spectrophotometer (Shimadzu UV 2450). The molar extinction coefficient (ε_{max}) was determined to be 4.0×10^4 $(cm \cdot mol/l)^{-1}$. The experiment was repeated for chosen samples as well as for the commercially-available titania nanomaterials, ST-01 (Ishihara Sangyo Kaisha, Ltd., Japan), which were tested for the sake of comparison. The commercial TiO_2 nanomaterial was used in the as-received state without further treatment before investigations. No I_3^- formation was observed when the experiments were conducted in the dark or in the absence of the TiO_2 specimens.

Results and Discussion

A TEM image and a SAED pattern of the 0.5 mol% ZrO_2-doped TiO_2 nanocrystals are given in Fig. 1. As can be seen in this figure, aggregates of nanoparticles were observed. The size of the anatase-type TiO_2 nanocrystals decreased from about 10-20 nm for undoped TiO_2 nanocrystals prepared by SATM [21], to about 7-15 nm for the 0.5 mol% ZrO_2-doped TiO_2 nanocrystals. It is obvious that the crystallite growth is suppressed by the presence of ZrO_2 as a guest metal oxide. Figure 2 gives XRD patterns of the 0.5 mol% ZrO_2-doped TiO_2

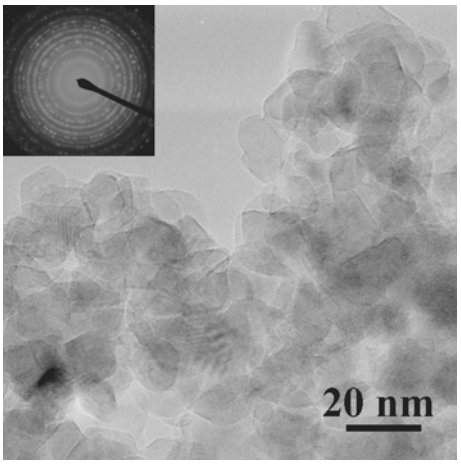

Fig. 1. TEM image of the 0.5 mol% ZrO_2-doped TiO_2 nanocrystals (inset; SAED of nanocrystals) calcined at 500°C.

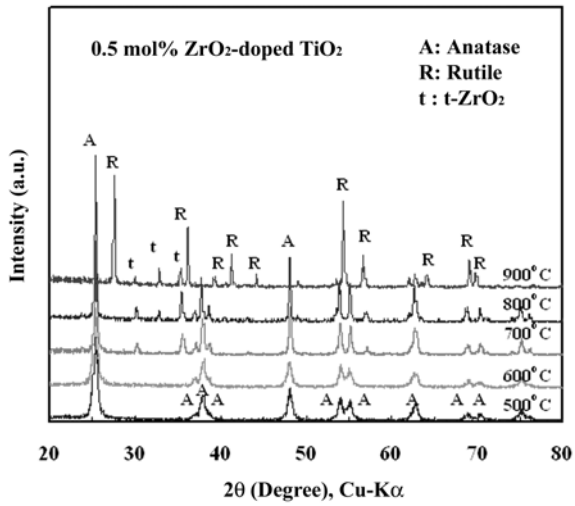

Fig. 2. XRD patterns of the 0.5 mol% ZrO_2-doped TiO_2 nanocrystals prepared by SATM.

nanocrystals derived from [ACA]/[Ti+Zr]=1, [LAHC]/[Ti+Zr]=0.25, and calcined at different temperatures (500°C-900°C) in air. It has been reported that fine anatase-type TiO_2 transforms to the rutile phase after calcination at 550°C-650°C [27, 28]. The XRD patterns revealed that the addition of ZrO_2 to TiO_2 tends to inhibit the phase transformation from the anatase to the rutile phase of TiO_2. Figure 3 shows representative examples of UV-vis diffuse reflectance spectra of the undoped TiO_2 and the 0.5 mol% ZrO_2-doped TiO_2 nanocrystals compared with that of ST-01 (equi-axed fine anatase particles, consisted of anatase). The absorption edge of the undoped TiO_2 (mesoporous anatase-type) by SATM calcined at 500°C occurs at ~380 nm, and its band gap energy is estimated to be about 3.26 eV. Meanwhile, the absorption edge of the 0.5 mol% ZrO_2-doped TiO_2 is slightly shifted by ~8 nm to a longer wavelength in comparison with that of the undoped TiO_2 nanocrystals. By adding ZrO_2, the value of the band gap is found to become slightly

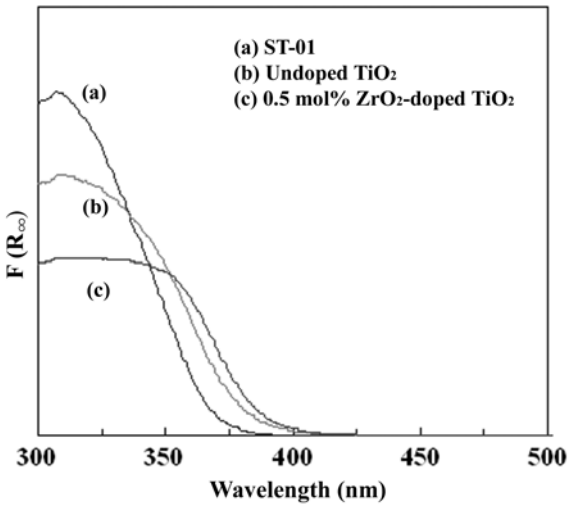

Fig. 3. UV-vis diffuse reflectance spectra of (a) ST-01, (b) undoped TiO_2 by SATM, and (c) 0.5 mol% ZrO_2-doped TiO_2 nanocrystals by SATM.

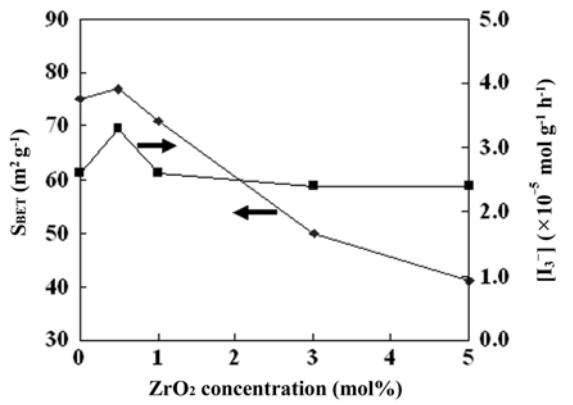

Fig. 4. Surface area and photocatalytic activity of the ZrO_2-doped TiO_2 nanocrystals (calcination temperature: 500°C) for different dopant concentration (in mol%).

lower than that of the undoped TiO_2, and with a slight decrease in energy band gap value.

The photocatalytic activity of the above mentioned mesoporous ZrO_2-doped TiO_2 nanocrystals were evaluated based on the formation of triiodide (I_3^-) species in a suspension of the TiO_2-based photocatalyst in KI aqueous solution after UV-irradiation. The surface area and the photocatalytic activity (estimated as a concentration of I_3^- in 10 ml of 0.2 M KI solution per unit mass of TiO_2 powder), for different dopant concentrations are depicted in Fig. 4. These results revealed that the photocatalytic activity and S_{BET} increased up to 0.5 mol% ZrO_2 doping and decreased for further dopant concentrations. It is considered that the 0.5 mol% ZrO_2-doped TiO_2 should have improved photocatalytic activity due to the rather high S_{BET} and small crystallite size in the presence of dopant species [7]. The photocatalytic reaction occurs on the surface of the TiO_2 catalyst during UV illumination and the recombination of photogenerated electrons and holes is very

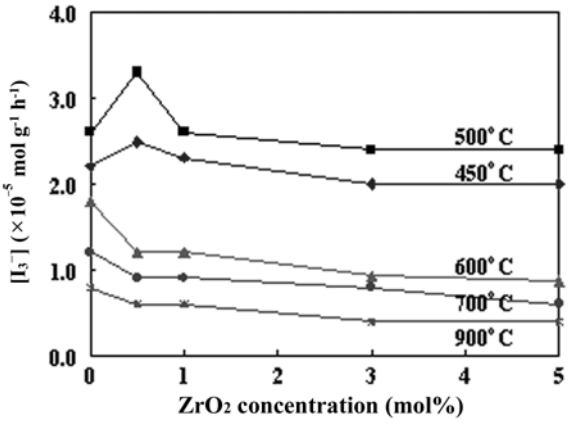

Fig. 5. The effect of calcination temperatures (450°C-900°C) on the photocatalytic activity of 0.5 mol% ZrO_2-doped TiO_2 nanocrystals.

fast [29]. The small amount of ZrO_2 may inhibit the electron-hole pair recombination and cause the enhancement of the photocatalytic activity. Although the photocatalytic activity of the 0.5 mol% ZrO_2-doped TiO_2 nanocrystals was ~30% lower than that of ST-01 tested under similar condition (5.0×10^{-5} mol·g^{-1}h^{-1}), the small amount of ZrO_2 addition itself should be a promising way to improve the photocatatlytic activity of TiO_2. The ZrO_2 content dependence of the photocatalytic activity for the ZrO_2-doped TiO_2 with different calcination temperatures (500°C-900°C) is shown in Fig. 5. It is obvious that the 500°C calcined nanocrystals exhibited the highest photocatalytic activity of all the ZrO_2 contents, which was attributed to the higher S_{BET}, and crystallinity. At calcination temperatures of 450°C-500°C, the 0.5 mol% doping showed maximum values. A vary small amount of ZrO_2 doping may contribute to enhance the crystallinity of TiO_2 [16] and inhibit the electron-hole recombination, and hence improve the photocatalytic activity. At temperatures higher than 500°C, all ZrO_2-doped TiO_2 nanocrystals exhibited lower photocatalytic activity than that of undoped TiO_2, due to the existence of the tetragonal ZrO_2 phase found on bulk powder [30], as shown in Fig. 2.

Conclusions

For mesoporous TiO_2 nanocrystals prepared by SATM, a small amount of ZrO_2 doping (0.5 mol%) improved the photocatalytic activity. ZrO_2 doping played a role in retarding the phase transformation from the anatase phase to the rutile phase of TiO_2 nanocrystals during calcining at various calcination temperatures and increased crystallinity with a reduced crystallite size. The photocatalytic activity of synthesized ZrO_2-doped TiO_2 nanocrystals greatly depends on the concentration of ZrO_2 and calcination conditions. The small amount ZrO_2-doped TiO_2 nanocrystals will be a key technique to have a high

surface area and small crystallite to enhance the photocatalytic activity of TiO_2.

Acknowledgements

This work has been supported by the 21COE program "Establishment of COE on Sustainable Energy System", and "Nanotechnology Support Project" of the Ministry of Education, Science, Sports, and Culture of Japan. The authors wish to thank Professor Seiji Isoda, Professor Hiroki Kurata, and Professor Toshinobu Yoko of the Institute for Chemical Research, Kyoto University, for the use of apparatuses. We also thank Dr. Yoshikazu Suzuki for helpful discussions.

References

1. W. Guo, Z. Lin, X. Wang, and G. Song, Microelec. Eng. 66 (2003) 95-101.
2. M.R. Hoffmann, S.T. Martin, W. Choi, and D.W. Bahnemann, Chem. Rev. 95 (1995) 69-96.
3. A. Fujishima and K. Honda, Nature 238 (1972) 37-38.
4. P.A. Mandelbaum, A.E. Regazzoni, M.A. Blesa, and S.A. Bilmes, J. Phys. Chem. B 103 (1999) 5505-5511.
5. M.A. Fox and M.T. Dulay, Chem. Rev. 93 (1993) 341-357.
6. L. Saadoun, J.A. Ayllón, J. Jiménez-Becerril, J. Peral, X. Domènech, and R. Rodríguea-Clemente, Appl. Catal. B: Environ. 21 (1999) 269-277.
7. Y. Zhang, G. Xiong, N. Yao, W. Yang, and X. Fu, Catal. Today 68 (2001) 89-95.
8. A. Di Paola, G. Marcì, L. Palmisano, M. Schiavello, K. Uosaki, S. Ikeda, and B. Ohtani, J. Phys. Chem. B 106 (2002) 637-645.
9. C. Karunakaran, S. Senthilvelan, S. Karuthapandian, and K. Balaraman, Catal. Commun. 5 (2004) 283-290.
10. J.C. Yu, J. Lin, D. Lo, and S.K. Lam, Langmuir 16 (2003) 7304-7308.
11. G. Sivalingam, K. Nagaveni, M.S. Hegde, and G. Madras, Appl. Catal. B: Environ. 45 (2003) 23-38.
12. H. Hahn and R.S. Averback, Nanostruc. Mater. 1 (1992) 95-100.
13. H. Yin, Y. Wada, T. Kitamura, S. Kambe, S. Murasawa, H. Mori, T. Sakata, and S. Yanagida, J. Mater. Chem. 11 (2001) 1694-1703.
14. M.K. Akhtar, S. Vermury, and S.E. Pratsinis, Nanostruc. Mater. 4 (1994) 537-544.
15. Yu. V. Kolen'ko, V. D. Maximov, A. A. Burukhin, V. A. Muhanov, and B. R. Churagulov, Mater. Sci. Eng.: C. 23(6-8) (2003) 1033-1038.
16. K.Y. Jung and S.B. Park, Mater. Lett. 58 (2004) 2897-2900.
17. Y.R. Do, W. Lee, K. Dwight, and A. Wold, J. Solid State Chem. 108 (1994) 198-201.
18. X. Fu, L.A. Clark, Q. Ying, and M.A. Anderson, Environ. Sci. Technol. 30 (1996) 647-653.
19. R.N. Viswanath and S. Ramasamy, Colloids Surf. A 133 (1998) 49-56.
20. D. Das, H.K. Mishra, A.K. Dalai, and K.M. Parida, Appli. Catal. A: Gen. 243 (2003) 271-284.
21. S. Sakulkhaemaruethai, Y. Suzuki, and S. Yoshikawa, J. Ceram. Soc. Jpn., 112 (2004) 547-552.
22. S. Sakulkhaemaruethai, Y. Suzuki, and S. Yoshikawa, J. Jpn. Soc. Powder Powder Metallurgy, 51 (2004) 789-794.
23. J. Augustynski, Electrochim. Acta 38 (1993) 43-46.
24. M. Adachi, Y. Murata, H. Harada, and S. Yoshikawa, Chem. Lett. (2000) 942-943.
25. G. Kortum, in "Reflectance Spectroscopy" (Springer-Verlag, 1969) p.22.
26. K.M. Reddy, S.V. Manorama and A.R. Reddy, Mater. Chem. Phys. 78 (2002) 239-245.
27. S.R. Yoganarasimhan and C.N.R. Rao, Trans. Faraday Soc. 58 (1962) 1579-1589.
28. J.C.S. Wu and C.-Y. Yeh, J. Mater. Res. 16 (2001) 615-620.
29. A.L. Linsebigler, G. Lu, and J.T. Yates, Jr., Chem. Rev. 95 (1995) 735-758.
30. M. Hirano, C. Nakahara, K. Ota, O. Tanaike, and M. Inagaki, J. Solid State Chem. 170 (2003) 39-47.